

## Formation and impact of hot spots on the performance of organic photovoltaic cells

Roland Steim, Stelios A. Choulis, Pavel Schilinsky, Uli Lemmer, and Christoph J. Brabec

Citation: *Applied Physics Letters* **94**, 043304 (2009); doi: 10.1063/1.3073857

View online: <http://dx.doi.org/10.1063/1.3073857>

View Table of Contents: <http://scitation.aip.org/content/aip/journal/apl/94/4?ver=pdfcov>

Published by the *AIP Publishing*

---

### Articles you may be interested in

[Current-voltage characteristics of organic photovoltaic cells following deposition of cathode electrode](#)  
*Appl. Phys. Lett.* **97**, 193307 (2010); 10.1063/1.3516469

[Influence of chemical doping on the performance of organic photovoltaic cells](#)  
*Appl. Phys. Lett.* **94**, 203306 (2009); 10.1063/1.3138131

[Control of open-circuit voltage in organic photovoltaic cells by inserting an ultrathin metal-phthalocyanine layer](#)  
*Appl. Phys. Lett.* **91**, 083518 (2007); 10.1063/1.2775085

[Semitransparent organic photovoltaic cells](#)  
*Appl. Phys. Lett.* **88**, 233502 (2006); 10.1063/1.2209176

[Numerical simulations of layered and blended organic photovoltaic cells](#)  
*Appl. Phys. Lett.* **86**, 164101 (2005); 10.1063/1.1901812

---

A promotional banner for Applied Physics Reviews. On the left is a cover image of the journal showing a diagram of a device structure. The background is a blue gradient with a bright light source on the right and a molecular model of blue spheres. The text 'NEW Special Topic Sections' is prominently displayed in white. Below it, 'NOW ONLINE' is in yellow, followed by 'Lithium Niobate Properties and Applications: Reviews of Emerging Trends' in white. The AIP logo and 'Applied Physics Reviews' are in the bottom right corner.

**NEW Special Topic Sections**

**NOW ONLINE**  
Lithium Niobate Properties and Applications:  
Reviews of Emerging Trends

**AIP** Applied Physics Reviews

# Formation and impact of hot spots on the performance of organic photovoltaic cells

Roland Steim,<sup>1,2,a)</sup> Stelios A. Choulis,<sup>3</sup> Pavel Schilinsky,<sup>1</sup> Uli Lemmer,<sup>2</sup> and Christoph J. Brabec<sup>1,a)</sup>

<sup>1</sup>Konarka Technologies GmbH, Landgrabenstr. 94, Nürnberg D-90443, Germany

<sup>2</sup>Light Technology Institute, Universität Karlsruhe (TH), Kaiserstr. 12, Karlsruhe D-76131, Germany

<sup>3</sup>Department of Mechanical Engineering and Materials Science and Engineering, Cyprus University of Technology, Limassol 3603, Cyprus

(Received 26 May 2008; accepted 5 January 2009; published online 27 January 2009)

The failure mechanisms of organic solar cells under reverse bias conditions were investigated. Localized inhomogeneities, so-called “hot spots,” leading to increased leakage currents under reverse bias, were identified as the dominant origin for failure. The intensity of hot spots does increase with the duration under reverse bias voltage. Cells with a higher leakage current density (i.e.,  $>100 \mu\text{A}/\text{cm}^2$  at  $-1 \text{ V}$ ) have a significant higher probability for dominant failure, while devices with low leakage current densities show less degradation under reverse bias stressing. © 2009 American Institute of Physics. [DOI: 10.1063/1.3073857]

Cost effective organic photovoltaics (OPVs) are a major building block in the future sustainable energy supply scenarios. The intense research and development efforts in that field, as measured by the number of publications and patents, increased significantly over the past 5 years and have led to efficiencies beyond 5%.<sup>1</sup>

For most applications, PV devices need to deliver higher voltages than a single cell can produce. This voltage is limited by the difference in the highest occupied molecular orbital of the doner and the lowest unoccupied molecular orbital of the acceptor material as well as the work functions of the interface materials. The module voltage can be increased by a factor of the number of used single cells connected in series. When an illuminated PV module is partially shaded, the shaded part becomes a load resistance for the rest of the circuit. In such an operation mode a shaded cell begins to consume electrical power instead of producing it. That electrical power generated by the illuminated part of the module then will drive the shaded cell in reverse bias. The diode characteristics of the shaded cell (i.e., in the third quadrant) then determines the overall power output characteristics of the partial shaded module and the severeness of degradation of the shaded part reported in this paper.<sup>2–8</sup>

We assume that shading of an organic solar cell module is equivalent to reverse biasing of a single cell. The solar cells were produced as reported earlier.<sup>9,10</sup> The active layer, consisting of a poly(3-hexylthiophene)/fullerene blended composite in a ratio of 1:1, was blade coated from xylene solutions on indium tin oxide coated polyethylene terephthalate (PET) substrates. These substrates were coated with either a poly(3,4-ethylenedioxythiophene):poly(strenesulfonate) (PEDOT:PSS) or a  $\text{TiO}_x$  layer, which form rectifying, selective interface contacts. Devices were than finished as either normal or inverted structures.<sup>10</sup> Active layers had a typical thickness of 250–280 nm. Results presented here are on inverted architectures exclusively. The current density-voltage ( $J$ - $V$ ) characteristics were measured with a

Keithley source measurement unit (SMU 2400). For illumination a calibrated Steuernagel solar simulator was used providing an AM 1.5G spectra at  $100 \text{ mW}/\text{cm}^2$ . To investigate the effect of reverse bias on flexible solar cells, we applied a negative bias of  $-5 \text{ V}$  under illumination of 1 sun and measured the  $J$ - $V$  parameters of devices before and after 5 h reverse bias degradation. The occurrence and growth of hot spots were monitored by a thermosensonic camera setup at the Bavarian Center for Applied Energy Research in Germany. A lock-in detection technique was used to guarantee highest temperature resolution.<sup>11,12</sup> The flexible solar cells were pulsed by a rectangle negative voltage of  $-5 \text{ V}$  at a frequency of 2 Hz. The spatially resolved heating of the cells due to different levels of energy dissipation was recorded by an infrared (IR) camera.

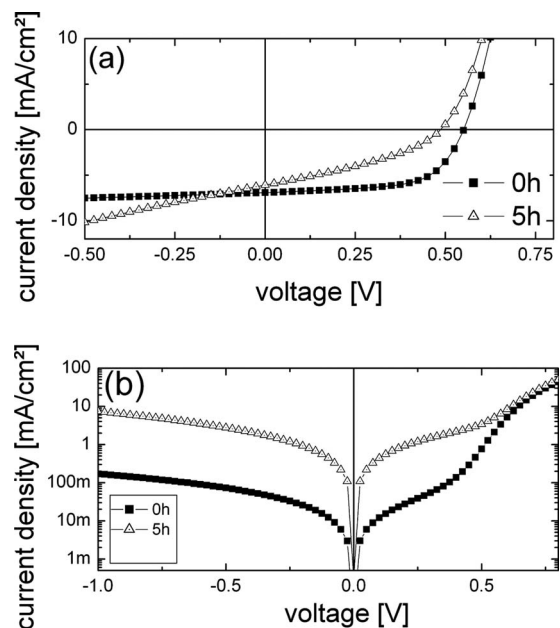


FIG. 1. Representative  $J$ - $V$  characteristics of the solar cell studied under illumination (a) and in the dark (b). The data are plotted in a linear-linear (a) and log-linear (b) representation.

<sup>a)</sup>Authors to whom correspondence should be addressed. Electronic addresses: rsteim@konarka.com and cbrabec@konarka.com.

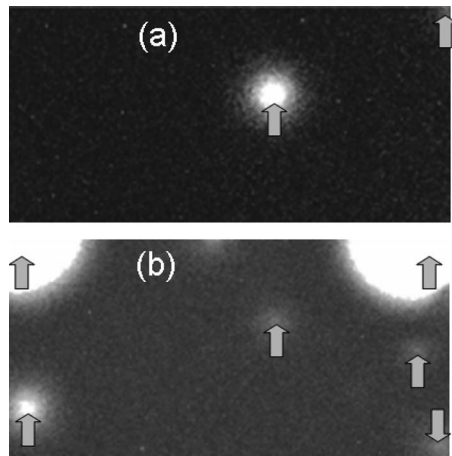


FIG. 2. IR emission measurement: image size represents active area of an organic solar cell of  $5 \times 10 \text{ mm}^2$ . Light colors correspond to higher temperatures than dark ones. (a) represents a thermosensory map of a nondegraded cell and (b) of a degraded cell. The color scale of each image was chosen to present the hot spots' qualitative best and is not fixed. The corresponding heat radiation to one color varies from measurement to measurement. Hot spots are marked by arrows as guides for the eyes.

Figure 1 presents a typical illuminated (a) and dark (b)  $J$ - $V$  curve of a flexible organic solar cell before and after reverse bias degradation. After 5 h at  $-5 \text{ V}$ , clear signs of degradation are observed. A small loss in the open circuit voltage ( $V_{oc}$ ) is accompanied by a dramatic loss in the electrical fill factor (FF). Such degradation is typical for the occurrence of shunts (low shunt resistance). Indeed, the dark  $J$ - $V$  curve proves this suspicion. The dark leakage current has increased by nearly two orders of magnitude after the reverse bias degradation. The short circuit current ( $J_{sc}$ ) is affected in the range of 10% from the initial value. The serial resistance is not affected. In summary, the increased leakage current is the most severe failure mechanism when reverse biasing an organic solar cell. In the following paragraphs we will investigate the origin of the increased leakage current.

We find that the severeness of degradation directly correlates with the power dissipation under reverse bias. In another set of experiments, the reverse current density was held constant, while the decrease in the applied voltage was monitored over time. Higher heat dissipation in the device, i.e., a higher product of voltage times current density, leads to significant faster degradation. This correlation also holds when fixing the applied bias to a constant negative value while monitoring the current density.

For imaging the heat dissipation, multiple cells were analyzed by high resolution IR measurements, and Fig. 2 presents a typical data set of a thermosensory measurement for an OPV cell before (a) and after (b) reverse bias degradation. These measurements clearly identify local areas with higher heat dissipation under reverse bias voltage, so-called hot spots, even for a nondegraded cell. For the specific cell under investigation and shown in Fig. 2(a), these spots are located on the edge as well as within the active area of the device. In Fig. 2(b) we show the thermosensory map of the organic solar cell after degradation under  $-5 \text{ V}$  reverse bias for 5 h. Reverse biasing of a cell significantly increased the amount of hot spots, which are detectable by the high sensitivity of the thermosensory setup ( $\mu\text{K}$  resolution). In addition, the amplitude signal of the existing hot spots, which is equivalent to the heat dissipated in the hot spots, increases

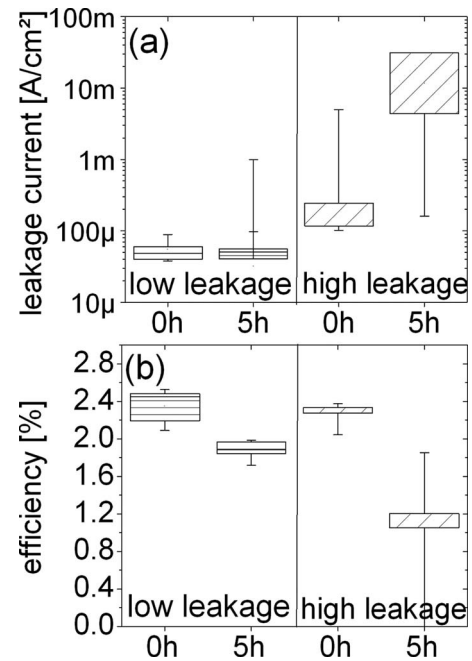


FIG. 3. Comparison of the degradation in dependent of the leakage current density. The upper plot (a) represents the leakage current at  $-1 \text{ V}$  before and after reverse biasing for 5 h at  $-5 \text{ V}$ . The cells are divided in low leakage current cells ( $<100 \mu\text{A}/\text{cm}^2$  at  $-1 \text{ V}$ ) and high leakage current cells ( $>100 \mu\text{A}/\text{cm}^2$  at  $-1 \text{ V}$ ). The plot beneath (b) presents the power conversion efficiency before and after reverse biasing for the high and low leakage current cells. Data are presented in box plots. The height of the box is the measurement for the tolerance.

under these conditions. Comparing the thermosensory map before and after degradation, it is safe to conclude that reverse biasing does induce increased local shunting (lower shunt resistance). In contrast to “dark spots” in organic light emitting diodes (OLEDs), we observed no passivation of the shunt in the middle of the hot spot.<sup>13</sup> On the other hand, similar to the dark spot formation in OLEDs, we observe that heat, dissipated at reverse bias in the hot spots, triggers further defect growth.

One can virtually divide the active area of the solar cell into little slices and assign each slice (“each single solar cell”) to an equivalent circuit, with all the slices connected in parallel. A slice consists of the semiconductor layer, the interlayer’s and the electrode materials. The discussion can be transferred to single layers in analogy. The reverse bias voltage applied on each slice is the same, irrespective of the electrical properties of the single slices. A slice with a higher local shunt (lower shunt resistance) will consequently result in higher local currents through the shunt. Since the heat dissipation is proportional to  $j^{2*}R$ , the reduction in the shunt resistance  $R$  in parallel to an increase in the Ohmic leakage current density  $j$  leads to an absolute increase in dissipated heat in and around the shunt, which causes further defect growth.

These results suggest that devices with no or only weak hot spots suffer from less degradation under reverse bias. That question is answered by plotting the degradation of devices in relation to their “time zero” shunts. Figure 3 compares the reverse bias degradation behavior of various cells with different magnitudes of leakage current, but otherwise identical. Before degradation, the cells are separated in two classes—one with a higher leakage current density

(>100  $\mu\text{A}/\text{cm}^2$  at  $-1$  V) and one with a low leakage current density (<100  $\mu\text{A}/\text{cm}^2$  at  $-1$  V) [see Fig. 3(a)]. Figure 3(b) compares the power conversion efficiency of the solar cells before and after reverse biasing at  $-5$  V for 5 h. A direct correlation between the leakage current density at time zero and the strength of degradation under reverse bias is found. Cells with a high initial leakage current density (>100  $\mu\text{A}/\text{cm}^2$  at  $-1$  V) have a significantly higher probability of severe degradation by more than 50% in efficiency under reverse bias stressing. These cells typically suffer from a strong increase in the leakage current (larger shunt), which is directly related to a dominant loss in the FF. On the other hand, cells with a low leakage current density (<100  $\mu\text{A}/\text{cm}^2$  at  $-1$  V) have a much higher probability to survive reverse bias stressing with only little degradation. Statistically, we find that the leakage currents of these cells do not increase, and, on the average, these cells lose less than 20% in performance after reverse biasing. The residual losses are mainly due to a slight decrease in FF and  $J_{\text{sc}}$ , with the FF losses being much lower ( $\sim 10\%$ ) compared to cells with high leakage current densities ( $\sim 40\%$ ). Most importantly we observe that cells with a sufficient low leakage current at time zero do not suffer from severe degradation. The increase in the leakage current and thus decrease in the FF is the dominant failure under reverse bias stressing. Cells with sufficient intact electrode interfaces and bulk layers do not develop new shunts during degradation. Contrarily, cells with interface or bulk defects rapidly degrade under reverse bias stressing due to an increase in the leakage current and a reduction in the FF.

We observed the same trend for different device architectures, including “normal” noninverted cells as well as for various interface and bulk materials. Thus the presented degradation mechanism does not appear to be limited to the presented device structure and material combination.

In summary we find a dominant contribution of local “high shunt” areas, so-called hot spots, to the degradation of bulk heterojunction solar cells under reverse bias. We find that the leakage current of an organic solar cell is a key parameter to control the dominant FF degradation under reverse bias stressing. Cells with sufficient low leakage currents at time zero remain stable over 5 h under reverse bias

stressing at a negative bias of ten times the  $V_{\text{oc}}$ . This is equivalent to a shading test for a ten stripe module, and it is safe to conclude that a ten stripe OPV module with a cell leakage current of <100  $\mu\text{A}/\text{cm}^2$  will show no or only little degradation under 5 h of shading. A further reduction in the leakage current, for instance, by improving the quality of the interfaces and the bulk layer, a further increase in reverse bias stability is expected.

Work of S.A.C. is performed at Konarka Technologies GmbH.

- <sup>1</sup>W. Ma, C. Yang, X. Gong, K. Lee, and A. J. Heeger, *Adv. Funct. Mater.* **15**, 1617 (2005); Y. Kim, S. A. Choulis, J. Nelson, D. D. C. Bradley, S. Cook, and J. R. Durrant, *Appl. Phys. Lett.* **86**, 063502 (2005); Y. Kim, S. Cook, S. M. Tuladhar, S. A. Choulis, J. Nelson, J. R. Durrant, D. D. C. Bradley, M. Giles, I. McCulloch, C.-S. Ha, and M. Ree, *Nature Mater.* **5**, 197 (2006); J. Y. Kim, K. Lee, N. E. Coates, D. Moses, T.-Q. Nguyen, M. Dante, and A. J. Heeger, *Science* **317**, 222 (2007); R. Gaudiana and C. J. Brabec, *Nat. Photonics* **2**; C. Hoth, S. A. Choulis, P. Schilinsky, and C. J. Brabec, *Adv. Mater. (Weinheim, Ger.)* **19**, 3973 (2007); C. J. Brabec, J. A. Hauch, P. Schilinsky, and C. Waldauf, *MRS Bull.* **30**, 50 (2005).
- <sup>2</sup>E. Molenbroek and D. W. Waddington, Conference Record of the IEEE Photovoltaic Specialists Conference, 1992 (unpublished), Vol. 1, pp. 547–552.
- <sup>3</sup>A. Woyte, J. Nijs, and R. Belmans, *Sol. Energy* **74**, 217 (2003).
- <sup>4</sup>M. C. García, W. Herrmann, W. Böhmer, and B. Proisy, *Prog. Photovoltaics* **11**, 293 (2003).
- <sup>5</sup>European Norm EN-61215, Crystalline silicon terrestrial photovoltaic (PV) modules—Design Qualification and Type Approval, 1995.
- <sup>6</sup>European Norm EN-61646, Thin-film terrestrial photovoltaic (PV) modules—Design Qualification and Type Approval, 1997.
- <sup>7</sup>UL1703, UL standard for safety for flat-plate photovoltaic modules and panels, 1993.
- <sup>8</sup>IEEE 1262, IEEE recommended practice for qualification of photovoltaic (PV) modules, 1995.
- <sup>9</sup>P. Schilinsky, C. Waldauf, and C. J. Brabec, *Adv. Funct. Mater.* **16**, 1669 (2006).
- <sup>10</sup>C. Waldauf, M. Morana, P. Denk, P. Schilinsky, K. Coakley, S. A. Choulis, and C. J. Brabec, *Appl. Phys. Lett.* **89**, 233517 (2006).
- <sup>11</sup>O. Breitenstein and M. Langenkamp, *Lock-in Thermography—Basics and Application to Functional Diagnostics of Electronic Components, Advanced Microelectronics* (Springer, Heidelberg, 2003), Vol. 10.
- <sup>12</sup>O. Breitenstein, J. P. Rakotoniaina, and M. H. Al Rifai, *Prog. Photovoltaics* **11**, 515 (2003).
- <sup>13</sup>L. Ke, S.-J. Chua, K. Zhang, and N. Yakovlev, *Appl. Phys. Lett.* **80**, 2195 (2002).